

OBSERVATIONS OF IN-SERVICE WEAR OF RAILROAD WHEELS AND RAILS UNDER CONDITIONS OF WIDELY VARYING LUBRICATION



TRANSPORTATION TEST CENTER
PUEBLO, COLORADO 81001

Interim Report

FRA/TTC-82/05

This document is available to the public through
The National Technical Information Service,
Springfield, Virginia 22161

PREPARED FOR
THE FAST PROGRAM

AN INTERNATIONAL GOVERNMENT - INDUSTRY RESEARCH PROGRAM

U.S. DEPARTMENT OF TRANSPORTATION
FEDERAL RAILROAD ADMINISTRATION
Washington, D.C. 20590

ASSOCIATION OF AMERICAN RAILROADS
1920 L Street, N.W.
Washington, D.C. 20036

RAILWAY PROGRESS INSTITUTE
801 North Fairfax Street
Alexandria, Virginia 22314



| | | | | | |
|--|--|--|---|---|-----------|
| 1. Report No. FRA/TTC - 82/05 | | 2. Government Accession No. | | 3. Recipient's Catalog No. | |
| 4. Title and Subtitle Observations of In-Service Wear of Railroad Wheels and Rails under Conditions of Widely Varying Lubrication. | | | | 5. Report Date July 1982 | |
| | | | | 6. Performing Organization Code | |
| 7. Author(s) Roger K. Steele | | | | 8. Performing Organization Report No. | |
| 9. Performing Organization Name and Address Transportation Test Center P.O. Box 11449 Pueblo, Colorado 81001 | | | | 10. Work Unit No. (TRAVIS) | |
| | | | | 11. Contract or Grant No. | |
| | | | | 13. Type of Report and Period Covered Interim Report | |
| 12. Sponsoring Agency Name and Address U.S. Department of Transportation Federal Railroad Administration FAST Program Washington, D.C. 20590 | | | | 14. Sponsoring Agency Code | |
| | | | | | |
| 15. Supplementary Notes *Federal Railroad Administration, Transportation Test Center, Pueblo, Co. Issued by: The FAST Program, Transportation Test Center | | | | | |
| 16. Abstract Some of the wheel and rail wear results from the current test at the Facility for Accelerated Service Testing are analyzed in the light of both adhesive and fatigue wear theories. This analysis suggests that the wheel:rail wear processes occurring in the unlubricated state are affected by more than one wear mechanism. Increases in the hardness of one component may cause an increase <u>or</u> decrease in the wear rate of the mating component. Which alternative does occur appears to be related to the mechanism of wear, the magnitude of the change in hardness, and the relative change in the wear rate of the component changed in hardness. A metallurgy:lubrication interaction that has been observed to occur when lubrication is applied had been found to be consistent with a concept of friction-dependent alteration of surface contact stresses when modified by the inclusion of a material sensitive parameter, i.e., hardness. | | | | | |
| 17. Key Words Wheel flange wear, rail gage face wear lubrication, wear mode model, metallurgy:lubrication interaction | | | 18. Distribution Statement This document is available through the National Technical Information Service 5285 Port Royal Road Springfield, VA 22161 | | |
| 19. Security Classif. (of this report) Unclassified | | 20. Security Classif. (of this page) Unclassified | | 21. No. of Pages 32 | 22. Price |

NOTICE

This document reflects events relating to testing at the Facility for Accelerated Service Testing (FAST) at the Transportation Test Center, which may have resulted from conditions, procedures, or the test environment peculiar to that facility. This document is disseminated for the FAST Program under the sponsorship of the U. S. Department of Transportation, the Association of American Railroads, and the Railway Progress Institute in the interest of information exchange. The sponsors assume no liability for its contents or use thereof.

NOTICE

The FAST Program does not endorse products or manufacturers. Trade or manufacturers' names appear herein solely because they are considered essential to the object of this report.

PREFACE

The author is grateful to Mr. Sergei Guins for pointing out the factors that affect the relative wear exposure of wheels and rail. Most especially, the author must acknowledge the contribution of Professor E. Rabinowicz in developing the method of analysis employed in the treatment of wear data as a function of rail to wheel hardness ratio, and for pointing out how the total system wear could be estimated. His insights in preparing an initial consolidated plot of the data of W. E. Jamison and of P. Clayton have been invaluable in guiding this author in the analysis of the FAST data.

TABLE OF CONTENTS

| <u>Section</u> | <u>Page</u> |
|--|-------------|
| Excutive Summary | vii |
| 1.0 Introduction. | 1 |
| 2.0 FAST Test Results | 5 |
| 3.0 Analysis. | 9 |
| 4.0 Discussion. | 17 |
| 4.1 Wheel and Rail Wear. | 17 |
| 4.2 Cause of Metallurgy:Lubrication Interaction. | 23 |
| 5.0 Conclusions | 29 |
| References | 31 |

LIST OF FIGURES

| <u>Figure</u> | <u>Page</u> |
|---|-------------|
| 1 Diagram of FAST Track | 2 |
| 2 Hardness Profiles in a Wheel Flange | 8 |
| 3 Wear Rates as a Function of Hardness, Dry Regime. | 11 |
| 4 Wear Rates as a Function of Hardness, Lubricated Regime | 12 |
| 5 Wear Rates as a Function of Rail/Wheel Hardness Ratio, Dry Regime. | 13 |
| 6 Wear Rates as a Function of Rail/Wheel Hardness Ratio, Lubricated Regime | 14 |
| 7 Rail/Wheel Wear Rate Ratios as a Function of Rail/Wheel Hardness Ratio | 18 |
| 8 Conceptual Arrangement of Wear Rate Plots for Adhesive Wear and for FAST Data. | 19 |

LIST OF FIGURES CONTINUED

| <u>Figure</u> | <u>Page</u> |
|---|-------------|
| 9 Illustration of Changes in Wear Rates Resulting from Change in Wheel Type from U to C. | 21 |
| 10 Octahedral Shear Stress Contours at Three Different Levels of Friction Coefficient (19 kip Wheel Load: New Rail) | 24 |
| 11 Agreement Between Observed and Predicted Wear Rates | 27 |
| 12 Conceptual View of Change in Wear Mechanism as Friction Coefficient Changes. | 28 |

LIST OF TABLES

| <u>Table</u> | <u>Page</u> |
|---|-------------|
| 1 Rail Mix in High Rail of Each Curve | 3 |
| 2 Characteristics of Track Lubricant. | 4 |
| 3 Wheel Mix of Train. | 4 |
| 4 Rail Gage Face Wear Rates | 6 |
| 5 Wheel Flange Wear Rates, Cast Wheels/Dry Regime | 6 |
| 6 Rail Hardnesses | 7 |
| 7 Cast Wheel Hardnesses on Side of Rim, Wheels IV Experiment. | 7 |
| 8 Amount of Equivalent 5° Curve | 9 |
| 9 Constants of Wear Rate/Hardness. | 10 |

ACRONYMS

| | |
|---------|--|
| BHN | Brinell hardness number |
| EHD | elastohydrodynamic |
| FAST | Facility for Accelerated Service Testing |
| FM | figure of merit |
| MGT | million gross tons |
| TTC | Transportation Test Center |
| FHT | fully heat treated |
| HH | head hardened |
| HR | hardness ratio |
| Std | standard carbon |
| Cr Mo A | Chrome Molybdenum, A |
| HiSi | high silicon |
| SiCr | silicon chrome |

ABBREVIATIONS AND CONVERSION FACTORS

| | | | |
|--------|------------------------|---|--|
| 1°F | degree Fahrenheit | = | $[(\text{°F}-32) \frac{5}{9}] \text{°C}$ |
| 1 mi | mile | = | 1.6094 km |
| 1', ft | foot | = | 0.3048 m |
| 1", in | inch | = | 25.4 mm |
| μm | micrometer | | |
| 1 ton | | = | 0.907 metric ton |
| 1 Cr | 1 percent chromium | | |
| psi | pounds per square inch | | |
| 1 mi/h | | = | 1.6094 km/h |
| 1 MGT | | = | 0.0907 MGMg |
| 1 kip | kilopound | = | 453.59 kg |
| ksi | kips per square inch | | |
| kg | kilogram | | |

EXECUTIVE SUMMARY

The operation of the Facility for Accelerated Service Testing has been described along with the features of the current rail metallurgy experiment. Results from this experiment have confirmed the existence of a metallurgy:lubrication interaction which significantly reduces the relative gage face wear advantage of premium rails over standard carbon rail when lubrication becomes generous. The greatest improvement in dry wear resistance is achieved by SiCr head hardened rail which is approximately four times more resistant to gage face wear than is standard carbon rail.

In order to treat the topic of total rail/wheel system wear, wheel flange wear rates (inches/1,000 miles) have been converted to the same units as rail gage face wear rate (inches/MGT). This is done by considering the effect of train length and operating procedure on the relative exposure of wheels and rails to wear events. Using wear for both components in comparable units, the total system wear is examined as a functional rail/wheel hardness ratio. It is shown in this analysis that total system wear will vary far less than will the wear of the rail itself as the hardness of rail is changed relative to that of the wheels. The analysis also shows that the effect of increasing the hardness of wheels to change the wear rate of rails appears to depend upon the mechanism of wear.

An explanation for the occurrence of the metallurgy:lubrication interaction is developed on the basis of the change in surface octahedral shear stress state as a function of the coefficient of friction and the different susceptibility of different metallurgies to respond to this change in surface stress state.

The following type of relationship is proposed:

$$\text{Wear rate} = A + B (\tau_{\text{oct}} / H^{2.5})$$

where A and B are empirical constants, τ_{oct} is the estimated surface octahedral shear stress, and H is gage face Brinell hardness.

1.0 INTRODUCTION

The replacement of worn rails and wheels represents one of the major operating expenses facing U.S. railroads. Although the use of premium rails and wheels may improve the performance of individual components, it is not at all clear how the widespread introduction of premium products would affect the overall resistance of the system to wear. Laboratory studies by Jamison¹ and Kumar and Margasahayam² have suggested that the price of improving the wear performance of one component is diminished wear performance of the mating component. Other laboratory studies by Babb³ and Marich and Curcio⁴ suggest contrariwise that improvements in the wear performance of one component may lead to improvements in the wear performance of the mating component.

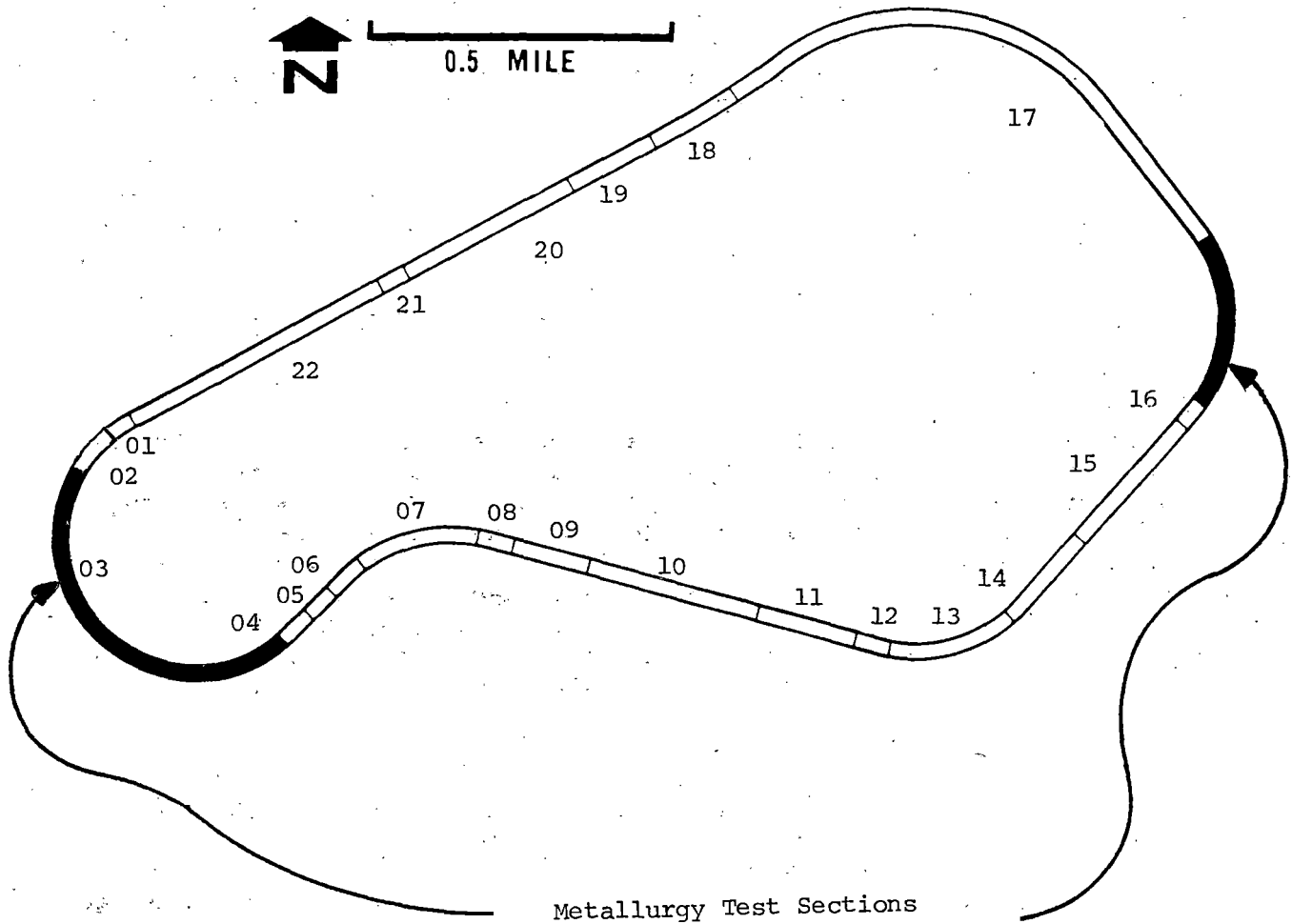
Following a format used by Rabinowicz in discussing wheel and rail wear for the AAR Material Advisory Committee, this report will present, compare, and analyze the wheel flange and the rail gage face wear behavior under the widely different lubrication conditions that are utilized in the current tests at the Facility for Accelerated Service Testing (FAST). The analysis will show how the FAST data may be used to estimate the wear of the mating component. A wear mode transition model is proposed to explain the observance of a metallurgy:lubrication interaction.

FAST is a 4.8 mi test loop at the Department of Transportation's Transportation Test Center (TTC), located near Pueblo, Colorado. A unit train of approximately 9,500 trailing tons (mainly loaded 100-ton capacity cars) makes about 100 laps around this test loop per day. This operation imposes approximately one million gross tons (MGT) of traffic per day on the track. The train travels about 500 to 600 mi per MGT, depending upon the length and weight of the train. The average train speed is 41 mi/h. The train reverses direction each day and the consist is turned every other day to insure a uniform exposure of the wheels to the rail. The configuration of the FAST loop is shown in Figure 1.

The rail population consists of standard AREA carbon rail, heat-treated rail, and alloy rail. The test rails are located in Section 03 (5°, timber ties) and in a 5° part of Section 17 (concrete ties). The types and quantities of rail in each curve (both test and nontest) are given in Table 1. Details of arrangement of the test rails and of measurement and analysis techniques have been described previously.⁵

In order to confirm the presence of an apparent metallurgy:lubrication interaction observed previously,⁵ an alternating pattern of lubricated and dry running was adopted in the current experiment. The lubricant used in the lubrication phase has been a graphite bearing grease having the characteristics given in Table 2. The lubricated phase has been interrupted every 2 to 3 MGT for periods of approximately 1/2 MGT to 'clean' the rail for flaw inspection. That is, the lubricated phase is not truly continuously lubricated.

¹ Numbers refer to the list of references.



Note: Numbers inside the loop are track section numbers.

FIGURE 1. DIAGRAM OF FAST TRACK.

TABLE 1. RAIL MIX IN HIGH RAIL OF EACH CURVE.

| Section | Curvature(°) | Overall Length(ft) | Length per Type of Rail (ft) | | | | | | | % Premium |
|---------|--------------|--------------------|------------------------------|-------|-------|----------|------|-----|------|-----------|
| | | | Std | FHT | HH | SiCr(HH) | CrMo | CrV | 1 Cr | |
| 03 | 5 | 3,670 | 935 | 200 | 935 | 400 | 800 | - | 450 | 76 |
| 07 | 5 | 1,000 | - | 1,000 | - | - | - | - | - | 100 |
| 13 | 4 | 1,250 | 1,250 | - | - | - | - | - | - | 0 |
| 17 | 5 | 1,300 | - | - | 200 | 400 | - | 400 | 300 | 100 |
| 17 | 3 | 2,126 | - | - | 2,126 | - | - | - | - | 100 |

Legend

- Std - standard carbon
- FHT - fully heat treated
- HH - head hardened
- SiCr (HH) - silicon chrome head hardened
- CrMo - chrome molybdenum
- CrV - chrome vanadium
- 1 Cr - 1% chrome

TABLE 2. CHARACTERISTICS OF TRACK LUBRICANT.

| | |
|-------------------------------------|--------|
| Penetration (worked) at 77° F | 340 |
| % Soap | 9 |
| % Graphite | 11.5 |
| Mineral Oil Viscosity (Centistokes) | |
| 100° F | 441 |
| 210° F | 53.6 |
| Dropping Point | 213° F |

In the current experiment, the wheels have been predominantly U (not heat treated) and C (heat treated) class wheels with a small portion of B (heat treated, lower carbon) class wheels. Table 3 presents the wheel mix of the complete train. Not all wheels in the train, though, were included in the wheel wear experiments.

TABLE 3. WHEEL MIX OF TRAIN.

| Lubrication Condition | Wheel Type(%) | | |
|-----------------------|---------------|---|----|
| | C | B | U |
| Dry | 43 | 2 | 55 |
| Lubricated | 76 | 2 | 22 |

2.0 FAST TEST RESULTS

The measure of rail wear is gage face wear; it is measured as lateral metal loss from that side of the high rail of the curve in contact with the wheel flange, 5/8" down from the current running surface of the rail. These rates* are summarized in Table 4. The relative merit of a premium metallurgy relative to standard rail tested under the same conditions diminished substantially as lubrication improved; i.e., a metallurgy:lubrication interaction existed. This is especially noticeable for SiCr rail (Table 4). When dry, the SiCr rail wore at about one-fourth the rate of standard rail, but when lubricated, the wear rate of SiCr was only 35% less than that of lubricated standard rail.

The wheel wear rate data^{6,7} are given in Table 5. At this time, wheel wear information is available only for the unlubricated period. The flange wear rate** of U wheels cited for the Wheels III experiment reflects 14,000 mi of running. That data cited in the Wheels IV experiment represent only 7,000 mi of running. As the Wheels IV experiment progresses, the flange wear rates of all wheel types are expected to decline somewhat further such that the wear rate of U wheels in the Wheels IV experiment will approach that cited for the Wheels III experiment. The Wheels IV results show that the C wheels wear at about 45% of the rate for U wheels in the unlubricated condition. This is in excellent agreement (41%) with observations made in earlier experiments.⁸

Brinell hardness numbers (BHN) have been obtained with a 3,000 kg load on the running surface and on the gage face of the test rails. The averages of these values are tabulated in Table 6. The design of the hardness tester prevented the determination of comparable Brinell hardnesses on the worn flanges of wheels, but micro hardness traverses⁹ made on a cross section of a FAST U wheel (Figure 2) suggest that the as-worn flange face may be about 20 BHN harder than the base wheel hardness. Table 7 presents the average side-of-rim hardnesses of the different wheels tested; the estimated as-worn flange hardness is taken to be 20 BHN higher.

* The wear measurements made upon both wheels and rails in the current experiment have utilized direct reading dial gage type instruments having a precision of 0.001" and long-term repeatabilities of about ± 0.003 ".

** Rate of lateral thinning of the wheel flange (inches/1,000 miles) measured 5/8" radially from the tread surface at the tape line.

TABLE 4. RAIL GAGE FACE WEAR RATES.

| Metallurgy | Dry (in/MGT) | Lubricated (in/MGT) | |
|--------------------------|-----------------|------------------------|------------|
| | | Section 03 | Section 17 |
| Standard | 0.0066 | 0.00100 | -- |
| Fully Heat-Treated | 0.0031 | 0.00070 | -- |
| Head Hardened | 0.0230 | 0.00075 | 0.00028 |
| Silicon Chrome | 0.0016 | 0.00065 | 0.00030 |
| Chrome Molybdenum (C) | 0.0029 | 0.00065 | -- |
| | (A) | 0.0036 | -- |
| Chrome Vanadium | 0.0027 | -- | 0.00040 |
| 1% Chrome | 0.0030 | 0.00065 | 0.00034 |

TABLE 5. WHEEL FLANGE WEAR RATES, CAST WHEELS/DRY REGIME.

| Experiment | Flange Wear Rate (in/1,000 mi) | Normalized Wear Rate (in/MGT) |
|---------------|-----------------------------------|----------------------------------|
| Wheels III | | |
| U (untreated) | 0.0140 | 0.0049 |
| C (treated) | 0.0063* | 0.0022 |
| Wheels IV | | |
| Sub U | 0.221 | 0.0070 |
| U | 0.174 | 0.0063 |
| B | 0.135 | 0.0049 |
| C | 0.090 | 0.0028 |

*Estimated for a C vs. U wheel figure of merit of 2.2 based upon a straight line drawn through the Wheels IV data plotted in Figure 5.

TABLE 6. RAIL HARDNESSES.

| Metallurgy | Mean Hardness (BHN) | |
|----------------------|---------------------|-----------|
| | Running Surface | Gage Face |
| Standard | 324 | 314 |
| Fully Heat Treated | 366 | 386 |
| Head Hardened | 355 | 381 |
| Silicon Chrome | 391 | 405 |
| Chrome Molybdenum, C | 344 | 353 |
| Chrome Molybdenum, A | 383 | 398 |
| Chrome Vanadium | 372 | 365 |
| 1% Chrome | 348 | 353 |

TABLE 7. CAST WHEEL HARDNESSES ON SIDE OF RIM, WHEELS IV EXPERIMENT.

| Class of Wheel | Average Brinell Hardness |
|----------------|--------------------------|
| Sub U | 249 |
| U | 273 |
| B | 295 |
| C | 317 |

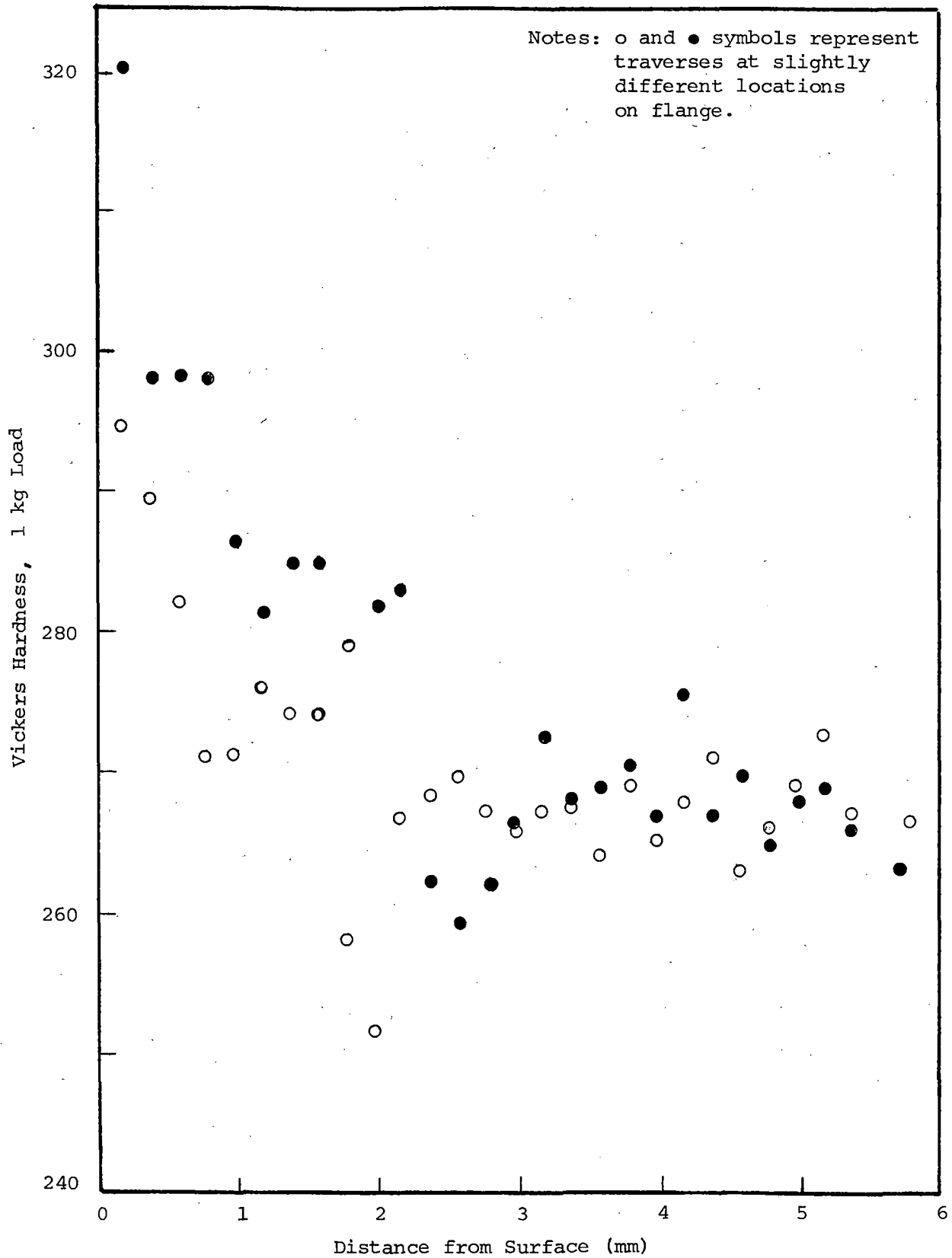


FIGURE 2. HARDNESS PROFILES IN A WHEEL FLANGE.

3.0 ANALYSIS

In order to relate the wear behavior of wheels to that of rail, it is necessary to convert wear rate to a comparable basis and to adjust for differences in exposure. As a first step, the 3° and 4° curves at FAST have been converted to equivalent 5° curves. This is done by recognizing that the relationship between rail wear and curvature is approximately linear up to about 5° curvature,⁵ so that 3° and 4° curves will produce respectively about 60% and 80% of the rail wear that a comparable 5° curve will produce. Thus the 9,346' of 3°, 4°, and 5° curvature in FAST reduces to a total of about 8,250' of equivalent 5° curvature. This is shown in Table 8.

TABLE 8. AMOUNT OF EQUIVALENT 5° CURVE.

| Section | Overall Length(ft) | Equivalent 5° Curve (ft) |
|---------|--------------------|--------------------------|
| 03 (5°) | 3,670 | 3,670 |
| 07 (5°) | 1,000 | 1,000 |
| 13 (4°) | 1,250 | 1,000 |
| 17 (5°) | 1,300 | 1,300 |
| (3°) | 2,126 | 1,276 |
| TOTAL | 9,346 | 8,246 |

The wheel does not see the same exposure to wear events as does the rail. In 8,250' of 5° curvature, a point on the flange of a 36" wheel (9.425' circumference) will undergo 875 wear exposures. In a 76 car, 4 locomotive train, 320 wheels will be exposed to the high rail. But if virtually all of the flange wear will occur on the high (outside) rail wheel of the leading axle in each truck,⁶ only one-half (160) of the high rail wheels will receive flange wear. In each lap, a site on the gage face of the high rail will see 160 wear events.

At FAST, the train reverses direction each day and the cars are turned every second day so that each wheel will see the high rail, lead axle wheel only once in every four days.

$$\frac{8,250'}{9,425'} \times \frac{1}{160} \times \frac{1}{4} \approx 1.4 \text{ times}$$

Thus the wheel sees ≈ 1.4 the exposure that the rail sees. If wheel wear rates in inches/1,000 mi were converted to inches/MGT (1,000 mi \approx 2 MGT) and if both wheel and rail had the same specific wear rate, the measured flange wear rate of wheels would be expected to be approximately 40% higher than that of rail. Here, the term 'specific wear' implies equal exposure for each half of the wear couple. The exposure factor varies with the length and weight of train along with the miles per MGT for each car. However, the exposure factor increases roughly in proportion to the miles per MGT so that on a specific wear basis, 1 MGT \approx 350 mi of travel.

With these relationships, it is now possible to place rail and wheel wear rates (determined at FAST only) on an equivalent basis. In Figure 3, the equivalent gage face and flange wear rates have been plotted semilogarithmically against Brinell hardness of the gage face or flange. The semilogarithmic function has been chosen because if the data were plotted on a linear basis and a single straight line were fitted through the data, zero wear rate would be predicted at hardness levels as low as 430 BHN for rail in the current experiment. Figure 3 presents the wear rate data in the unlubricated regime. The normalized wheel wear rates fall slightly below those of the rail as a group. The rail wear rate data of the generously lubricated regime are plotted in Figure 4; the dependency of wear rate on hardness is significantly reduced--a reflection of the metallurgy:lubrication interaction.

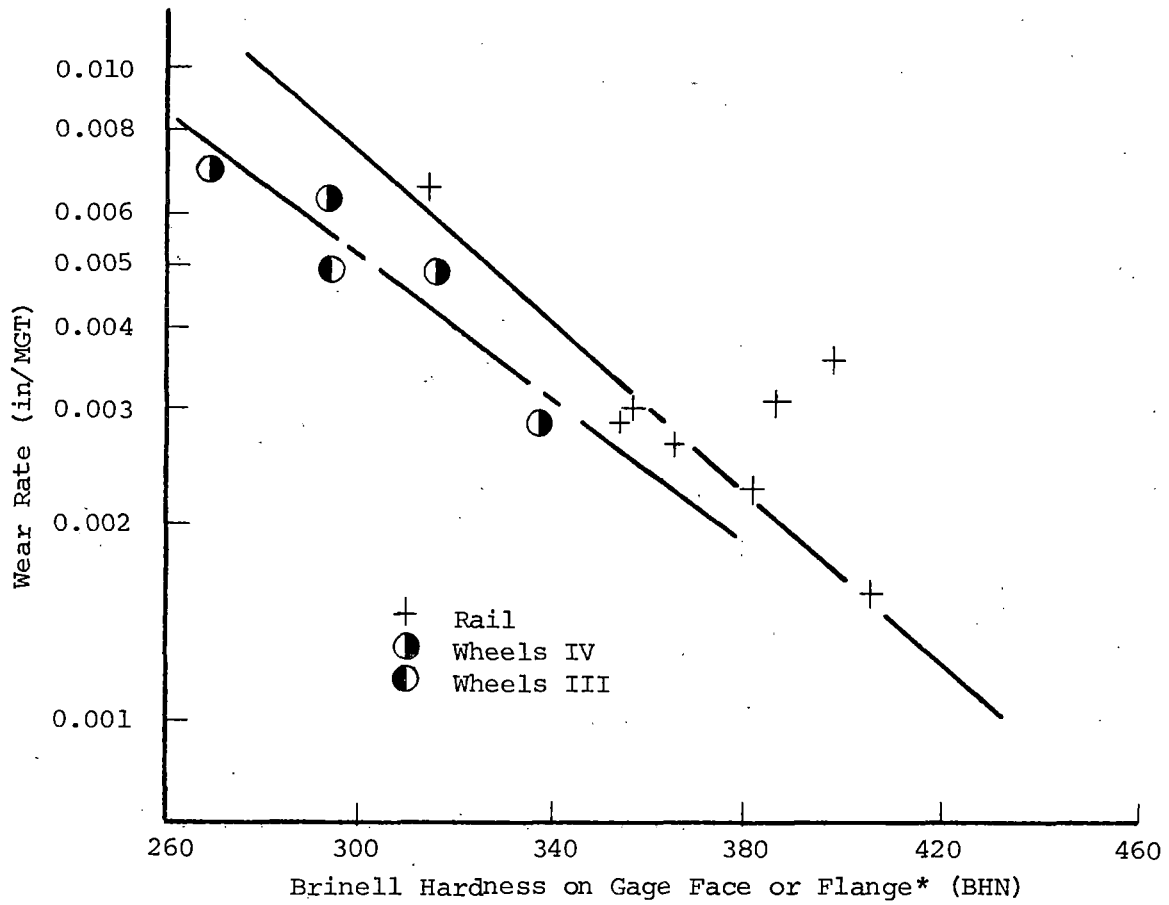
The general form of the wear rate (W):hardness (H) relationship is $\log W = A + B(H)$. The values of the constants are tabulated in Table 9.

TABLE 9. CONSTANTS OF WEAR RATE/HARDNESS.

| | | $\log W = A + B(H)$ | |
|---------|------------|---------------------|---------|
| | | A | B |
| Rail: | Dry | -0.014 | -0.0066 |
| | Lubricated | -2.253 | -0.0024 |
| Wheels: | Dry | -0.480 | -0.0059 |

Rabinowicz has pointed out¹⁰ that the wear of the hard and soft halves of a wear couple can be related to the ratio of the hardnesses of the two halves. Adopting this convention, Figures 5 and 6 illustrate the wear rate behavior as a function of the rail:wheel hardness ratio for unlubricated and lubricated regimes, respectively. The hardness ratio for each rail was calculated against the average hardness of the wheels; that for each wheel class was calculated against the average hardness of the rails. The average hardness of wheels was calculated from the average wheel mix in the train in the first lubrication/no lubrication block of the current experiment as,

$$\bar{H} = \sum n_i H_i$$



* Estimated value for flange is rim hardness + 20 BHN.

FIGURE 3. WEAR RATES AS A FUNCTION OF HARDNESS, DRY REGIME.

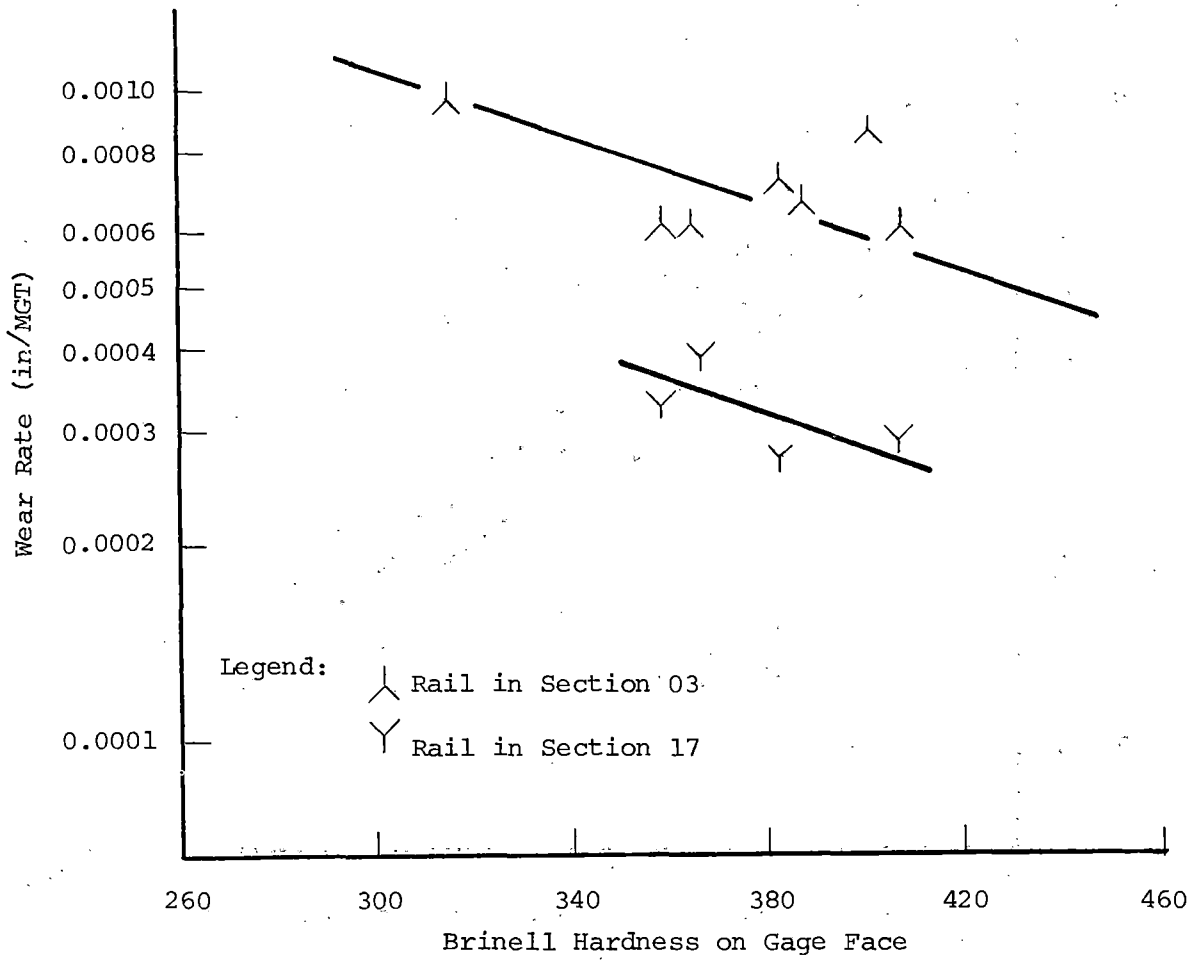
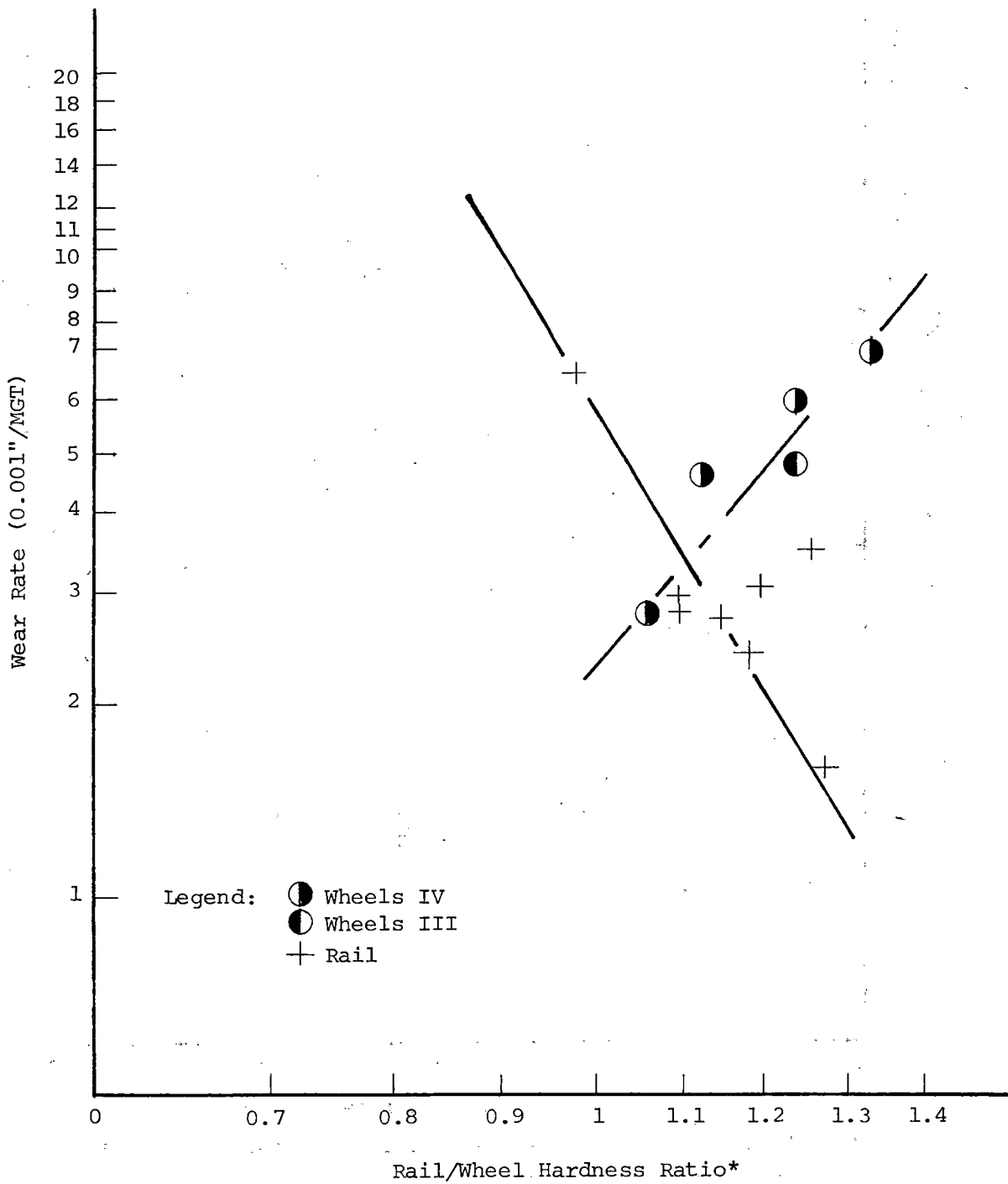
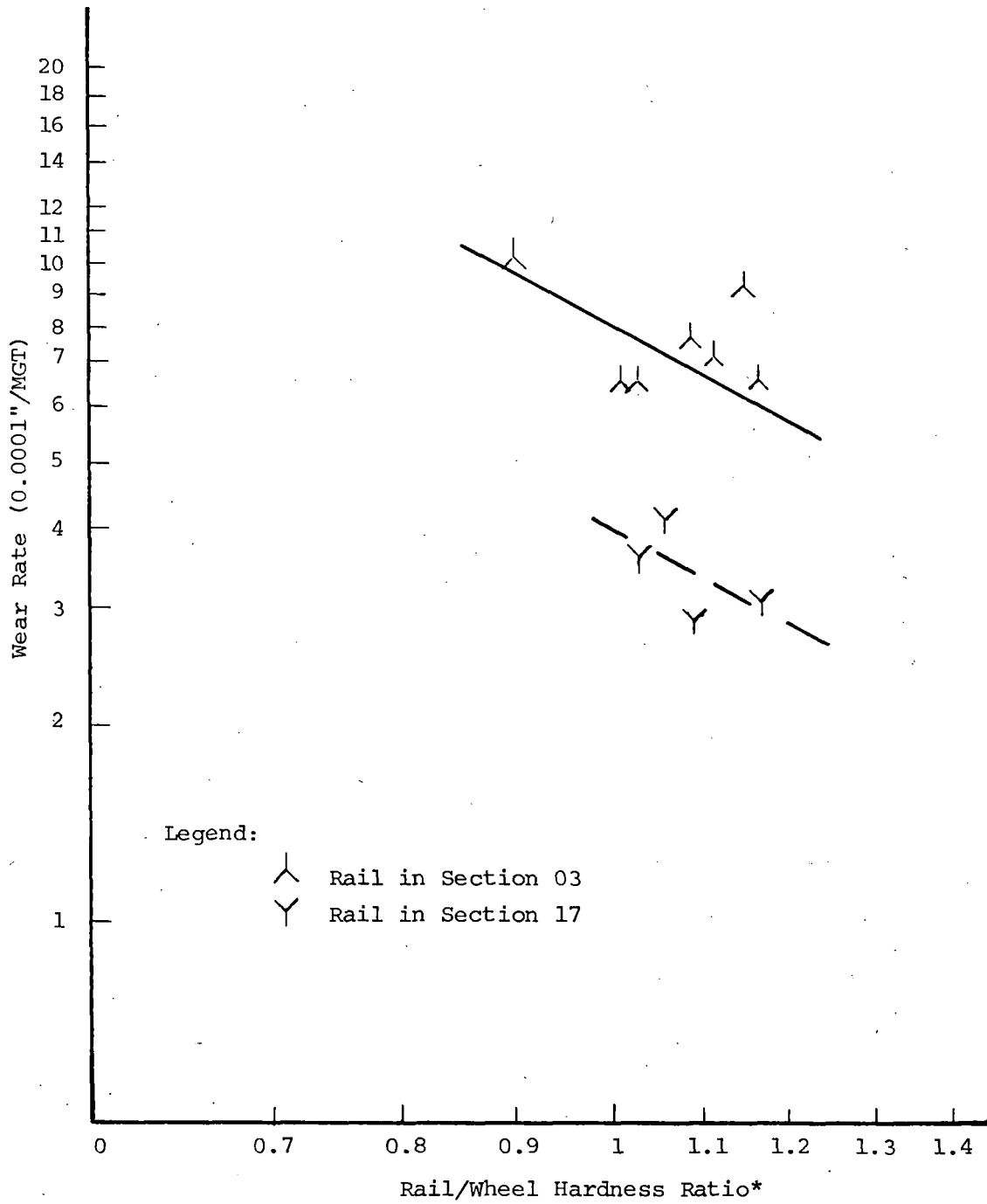


FIGURE 4. WEAR RATES AS A FUNCTION OF HARDNESS, LUBRICATED REGIME.



* Calculated as individual rail metallurgy average hardness \div mean wheel hardness, or mean rail hardness \div individual wheel hardness.

FIGURE 5. WEAR RATES AS A FUNCTION OF RAIL/WHEEL HARDNESS RATIO, DRY REGIME.



* Calculated as individual rail metallurgy average hardness \div mean wheel hardness.

FIGURE 6. WEAR RATES AS A FUNCTION OF RAIL/WHEEL HARDNESS RATIO, LUBRICATED REGIME.

where \bar{H} was the overall average hardness, n_i was the fraction of wheels of type i in the train, and H_i was the average estimated flange hardness of type i wheels. Average high rail hardness in the curves was calculated in the same way for each metallurgy i .

In the unlubricated regime (Figure 5), the slope of the rail plot is -5.9, while that for the wheels is near 4.0. In the lubricated regime (Figure 6), the rail slope (approximately -2) is significantly less than that observed in the unlubricated regime. However, the data from track Section 17 are a separate population below the data of track Section 03, although the slope of a line drawn through the data is about the same as that of Section 03 data.

4.0 DISCUSSION

To provide a consolidated presentation of relative wheel and rail wear performance and to permit comparison with observations from other sources, the rail/wheel wear rate ratios are plotted against the rail/wheel hardness ratios in Figure 7. This permits data sets with different units of measure to be compared on one figure. Because each rail sees the average of all the wheel flanges and each wheel flange sees the average of all the high rails in curved track, the FAST rail wear rates have been divided by the expected mean wear rate of the mix of U, B, and C wheels given in Table 3; and the rail:wheel wear rate ratios for wheels have been calculated by dividing the Wheels IV wear rates (Table 5) into the mean rail wear rate. In addition, data from laboratory tests by Marich and Curcio⁴ and Jamison¹ and field data by Clayton¹¹ of British Rail are shown. On such a plot as this, information shown by Rabinowicz¹⁰ suggests that a purely adhesive wear process should be characterized by a slope of -2 for rail/wheel hardness ratio greater than unity. The FAST data seem to have the same general disposition as the data of Clayton--neither of which are quite as steeply inclined as that of Jamison. These data sets have slopes greater than the -2 slope that is expected for an adhesive wear process. Interestingly, when the laboratory data of Marich and Curcio⁴ are plotted, the data set falls below the others but the slope is close to -2. There is some small uncertainty as to the appropriate hardness values to use in calculating the hardness ratio for the CrMo rail steel, but this uncertainty will not affect the slope strongly.

4.1 WHEEL AND RAIL WEAR

The observed behavior of FAST rail and wheels presented as plots of wear rate versus hardness ratio may be used to estimate component wear for different combinations of standard and premium products. To do this Rabinowicz¹² has proposed that the following assumptions are reasonable: a) The wear rate of the softer component of a wear couple will depend inversely on the first power of its hardness. Thus if the hardness of the wheel remains unchanged at rail:wheel hardness ratios greater than unity, the wheel wear rate would be expected to appear as a horizontal line to the right on the log-log axes of Figure 8. b) For essentially adhesive wear, the ratio of rail and wheel wear rates is related to the square of the hardness ratio. Thus the rail wear rate would be described by a straight line of slope -2 downward to the right. c) At the same hardness, the wheel and rail will have the same specific wear rates.

The FAST data as well as that of Clayton and Jamison suggest a slope nearer to -6, which implies a relationship between rail:wheel wear ratio and the hardness ratio raised to the sixth power. This greater dependence on hardness ratio suggests that some other mode of wear contributes to wear in addition to the adhesive component. At or about a hardness ratio of unity, the specific wear rates of both rail and wheel would be expected to be equal.

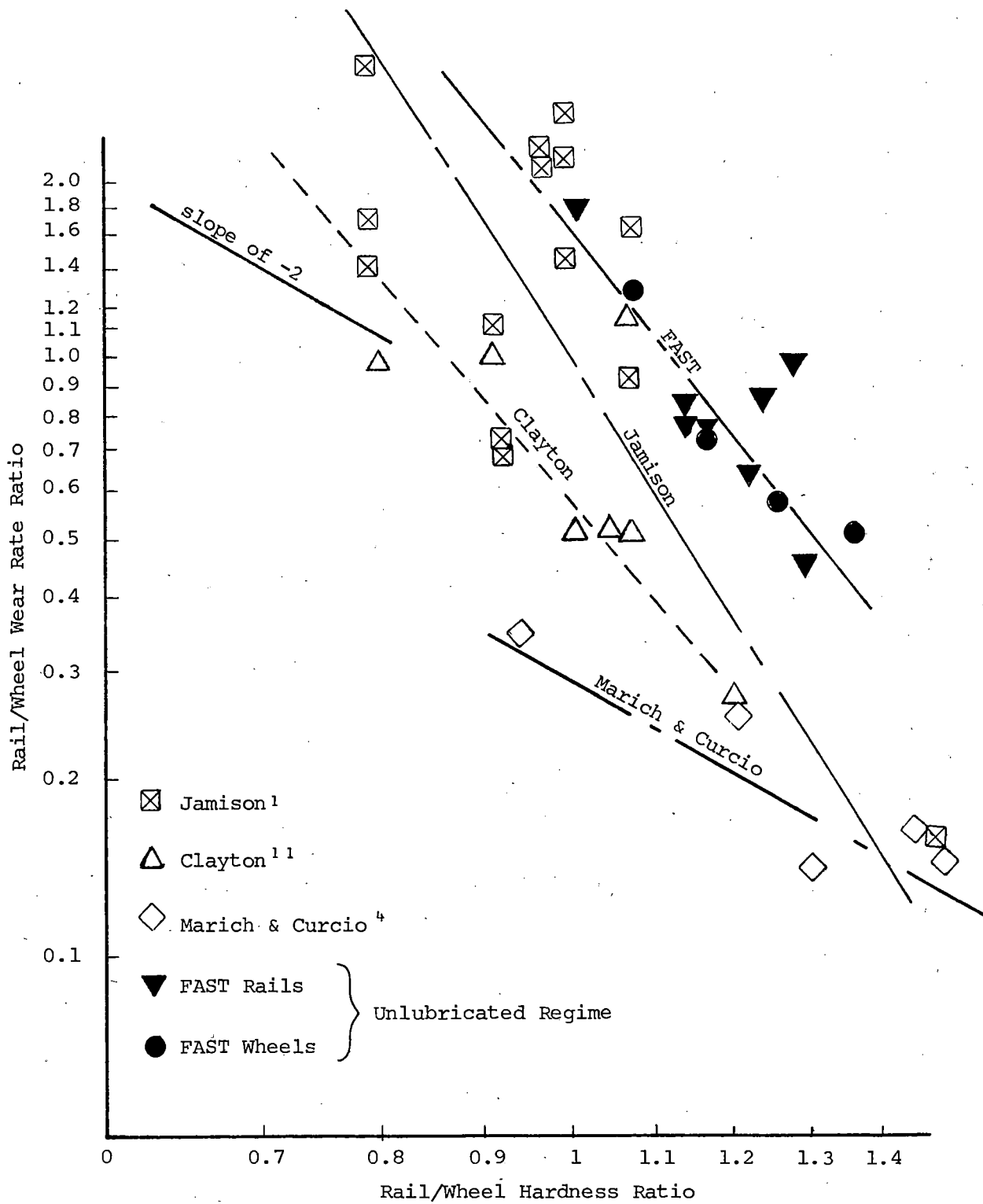


FIGURE 7. RAIL/WHEEL WEAR RATE RATIOS AS A FUNCTION OF RAIL/WHEEL HARDNESS RATIO.

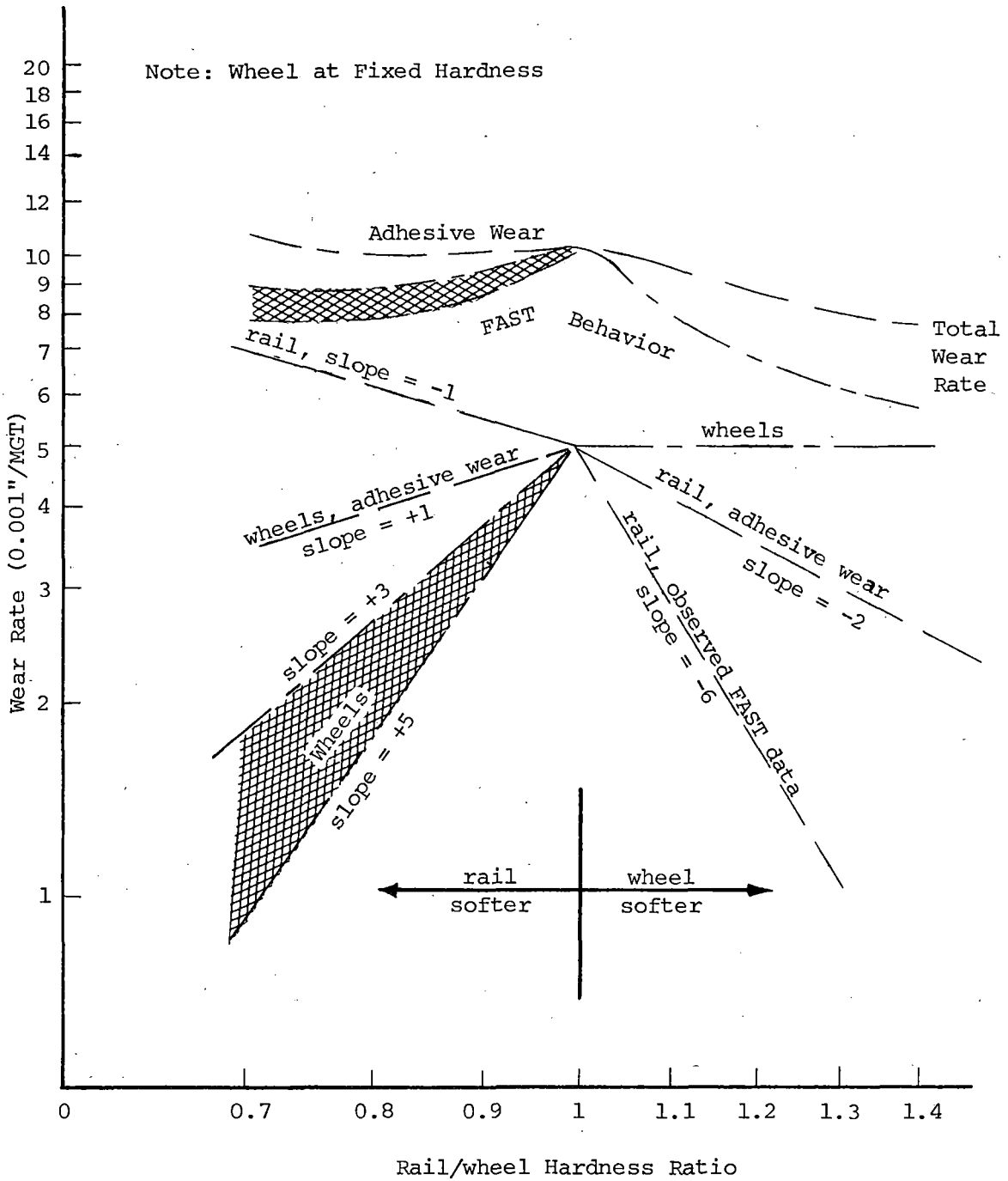


FIGURE 8. CONCEPTUAL ARRANGEMENT OF WEAR RATE PLOTS FOR ADHESIVE WEAR AND FOR FAST DATA.

At fixed wheel hardness and rail:wheel hardness ratios less than unity, the relationship between rail and wheel wear rates may be represented by a rail line sloped upward to the left and a wheel line sloped downward to the left. For essentially adhesive wear, the rail slope will be -1 and that for wheels will be +1. If the observed sixth power relationship observed at rail:wheel hardnesses greater than unity applied at ratios less than unity, the respective slopes would be -1 for rail and +5 for wheels such that algebraic sum of the slopes will be the same for all values of hardness ratio, i.e.,

$$\begin{array}{ll} -1 & -(+5) \\ \text{HR} < 1 & \text{HR} > 1 \end{array} \quad \begin{array}{ll} -6 & + 0 \\ \text{HR} < 1 & \text{HR} > 1 \end{array}$$

Similarly, if a fourth power relationship applied for wheel wear rate (as suggested by the wheel slope in Figure 5), the respective slopes would be -1 and +3. This presumes that the wear rate of the softer component (the rail now) is still inversely related to the first power of hardness.

The total system specific wear rate is the sum of the wheel and rail wear rates at each hardness ratio. These also are shown in Figure 8 for conditions of essentially adhesive wear and for the observed FAST wear behavior. If the rail wear rate is added to the wheel wear rate at individual hardness ratios between 0.7 and 1.4, the upper family of 'total wear rate' curves prevail. For essentially adhesive wear, a 2:1 increase in hardness ratio (from 0.7 to 1.4) will yield only a 27% reduction in total system wear rate, even though the rail will have exhibited a 64% decrease in wear rate and the wheel will have exhibited an approximately 50% increase in wear rate. For the actually observed FAST behavior, the maximum total wear rate would be expected to occur at a hardness ratio of unity, with the maximum reduction in system wear rate ($\approx 44\%$) occurring at hardness ratios greater than unity.

The slopes of the lines drawn in Figure 8 appear to depend predominantly on the mechanism of wear, which for small variations (less than 50%) in hardness ratio is assumed not to change significantly. However, the fact that the analysis which follows (Figure 9) shows a dissimilar behavior for Std and HH rail when U wheels are replaced with C wheels suggests that the slopes of Figure 5 could be affected somewhat by mating component hardness. The surface hardness of each component is expected to be relatively independent of the character of the mating surface.

If essentially adhesive wear occurred (rail line slope of -2), the U wheels (293 BHN) wearing at the observed (FAST) rate of $\approx 0.005"/\text{MGT}$ would be associated with a wear rate in HH rail (381 BHN) of about $0.003"/\text{MGT}$. An interesting observation results if the U wheels are replaced with C wheels (337 BHN), wearing at the expected (FAST) rate of $0.0022"/\text{MGT}$: the HH rail would be expected to exhibit a lower wear rate of about $0.0017"/\text{MGT}$. However, if the actually observed slope (-6) were used, the wear rate of HH rail would appear to increase very slightly.

A similar analysis is shown for Std rail (314 BHN); however, in this case the hardness ratio of Std rail running against C wheels will be less than unity. ~~Regardless of whether essentially pure adhesive wear or the observed (FAST) wear dependency on hardness ratio occurs, the change from softer U~~

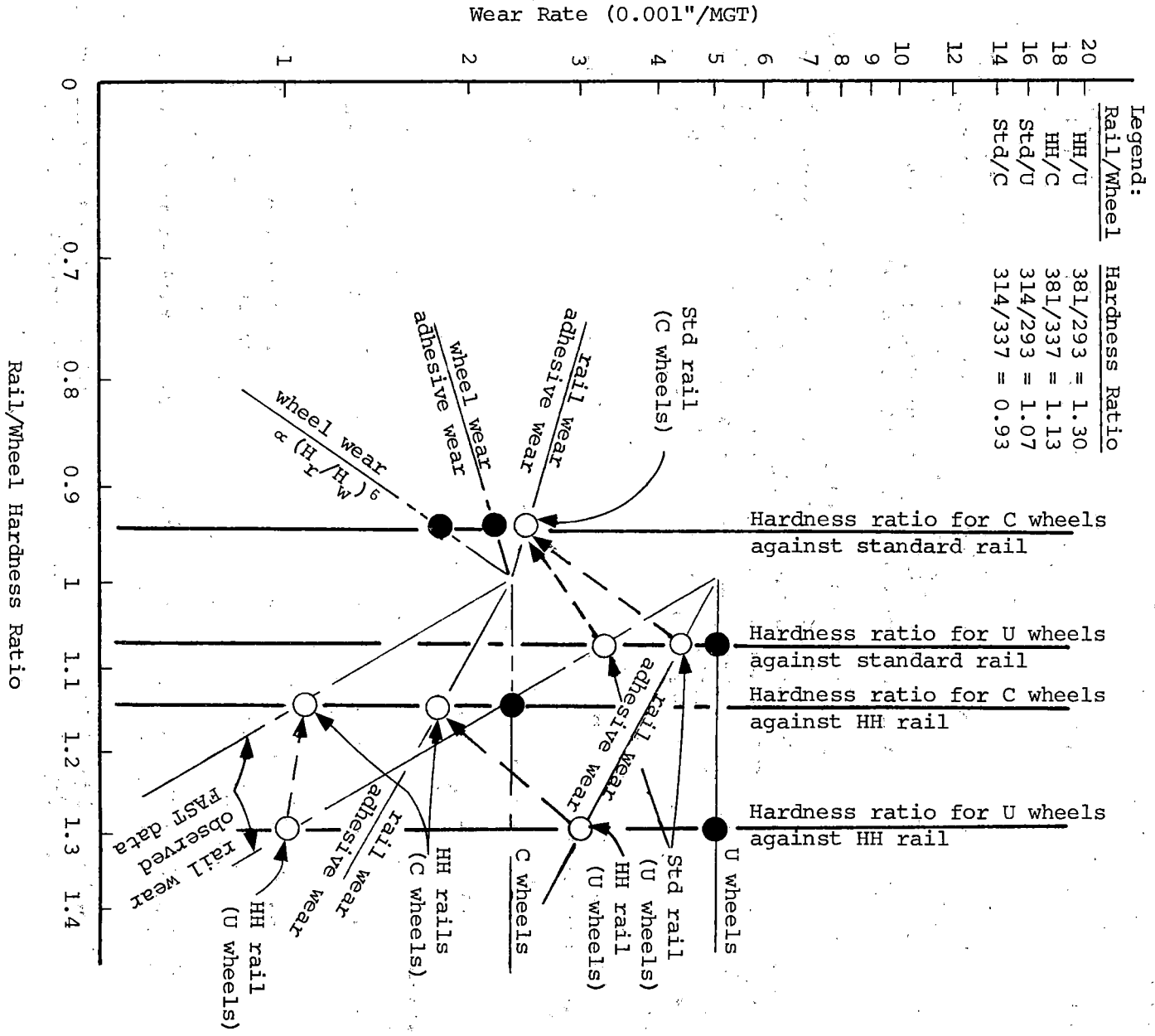


FIGURE 9. ILLUSTRATION OF CHANGES IN WEAR RATES RESULTING FROM CHANGE IN WHEEL TYPE FROM U TO C.

wheels to harder C wheels would appear to be accompanied by a decrease in the wear rate of the Std rail.

In the case of the observed (FAST) dependency, the expected changes in wheel and rail wear are small enough so that they might avoid detection on a statistically significant basis. However, the changes for a condition of essentially pure adhesive wear are large enough that they should be detected reliably. It is perhaps noteworthy (or coincidental) that the data of Marich and Curcio⁴ appear to exhibit a hardness ratio dependency close to that expected for essentially pure adhesive wear, and that these authors report that improvements in the wear performance of one component may lead to improvements in the wear performance of the mating component.

The analysis suggests that either improvement or deterioration of the wear performance of one component is possible by increasing the hardness of the mating component. Which will occur depends upon the mechanism of wear (dependency upon hardness ratio), the magnitude of the change in hardness, and the relative difference in wear rates of the component that is changed. This last factor can be considered a figure of merit which would be about 2.2 for C wheels relative to U wheels, calculated by dividing the wear rate of U wheels by that of C wheels.

This behavior may be described mathematically for U and C wheels in the following manner:

$$W_U = A_U (HR_U)^{n_U}$$

$$W_C = A_C (HR_C)^{n_C}$$

where,

W_U, W_C = the wear rate of the rail against U and C wheels, respectively,

A_U, A_C = a constant representing the point at which the rail and wheel wear rates are equal, i.e., at unity hardness ratio for U and C wheels, respectively,

HR_U, HR_C = the rail to wheel hardness ratio for rail against U and C wheels, respectively, and

n_U, n_C = the slope of the log-log rail wear rate versus hardness ratio plot for rail against U and C wheels, respectively.

For hardness ratios (HR) greater than unity, $n_U = n_C = n$. Also A_C will equal A_U/FM where FM is the figure of merit of C wheels relative to U wheels. Thus,

$$\frac{W_U}{W_C} = FM \left(\frac{HR_U}{HR_C} \right)^n$$

and the point at which a change from U wheels to C wheels will produce no change in rail wear rate will be at $W_U/W_C = 1$

$$\text{or } \left(\frac{HR_C}{HR_U} \right)^n = FM.$$

A question that cannot be answered at this time using the FAST data is whether the wear rate of the softer component really remains constant (at fixed hardness) as the mating component becomes harder.

4.2 CAUSE OF METALLURGY:LUBRICATION INTERACTION

Turning now from the relationship of wheel and rail wear, the possible cause of the observed metallurgy:lubrication interaction deserves some consideration. Jamison¹ proposed a mode transition from mild to severe wear under combined rolling and sliding with variations in humidity. Steele¹³ observed in a discussion of reference 1 that the same mechanism could be utilized to explain a metallurgy:lubrication interaction. The basis for such an explanation is the strong effect of friction coefficient (i.e., lubrication) on the surface stress state within the contact patch between wheel and rail.

Figure 10 illustrates the change in octahedral shear stress state that can occur at the running surface as the friction coefficient varies from zero to 0.5 at a 19 kip wheel load.¹⁴ A model that will explain the observed metallurgy:lubrication interaction must address two issues:

- The smaller relative variation in wear resistance under lubricated conditions among different metallurgies by comparison with that of the unlubricated state.
- The change in the response of wear rate to contact stresses as friction coefficient changes under constant flanging forces.

It is not clear how the vertical and lateral forces (developed on curving of the vehicle) are partitioned between the gage face and running surface of the rail. However, the fact that the gage face is typically as hard as the running surface (Table 6) suggests that both see comparable forces, and that analyses that predict the stress state on the running surface are also applicable (in a qualitative sense, at least) to the gage face.

Under full lubrication, a condition of elastohydrodynamic (EHD) lubrication is most likely to prevail, separating the mating components and preventing asperity contact. Wear occurring under this circumstance presumably would require a process that does not involve metal to metal contact.

Stone and Steele¹⁵ have proposed a fatigue model of wear that predicts qualitatively the types of variations in wear rate seen in the generously lubricated phase. The model predicts that wear rate would be proportional to the parameters:

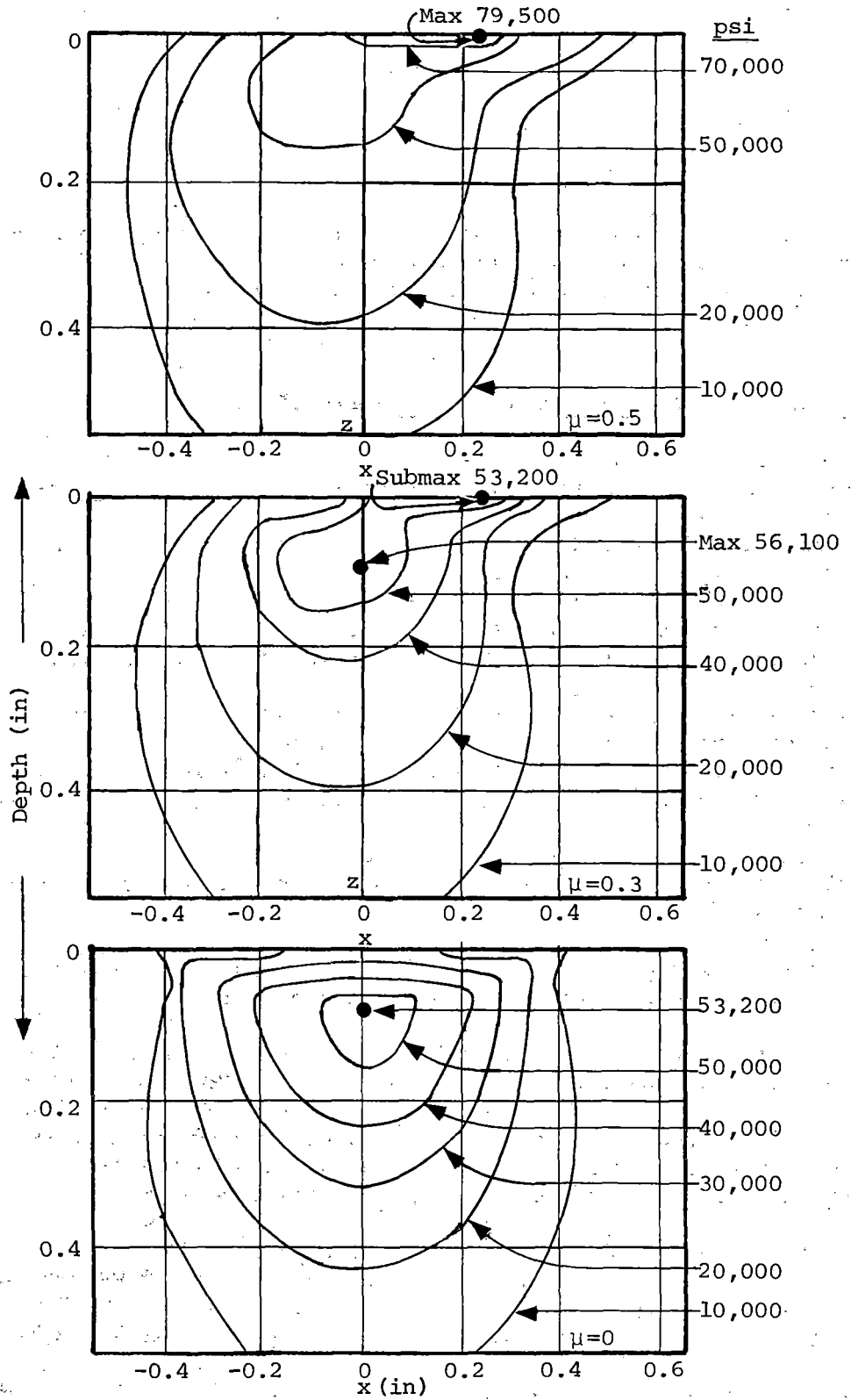


FIGURE 10. OCTAHEDRAL SHEAR STRESS CONTOURS AT THREE DIFFERENT LEVELS OF FRICTION COEFFICIENT (19 kip WHEEL LOAD: NEW RAIL).

$$\left(\frac{1}{P_f'}\right)^{-1/b} \text{ or } \left(\frac{1}{\epsilon_f'}\right)^{1+5n'}$$

where,

P_f' = the pressure equivalent of σ_f' , the cyclic fracture stress,¹⁶

b = the slope of the logarithm of applied stress against logarithm of twice the number of cycles to failure,

ϵ_f' = the cyclic fracture strain, and

n' = the cyclic work hardening exponent.

The only cyclic stress-strain data that seem to be available for rail compositions which are in test at FAST are for as-rolled UIC grade A (approximately standard AREA carbon rail) and 1 weight percent chromium (1 Cr) rail.¹⁷ Although the true static fracture strength of 1 Cr rail steel is about 20% greater than that of the UIC(A), the cyclic fracture strengths of the two metallurgies are virtually the same (1% different). However, the fatigue ductility coefficient, ϵ_f' , of 1 Cr is about 40% higher than that of UIC(A). Using an average b value of 0.094 for 1 Cr and UIC(A) rail, the 1 Cr rail should wear about 12% better than Std rail in the lubricated fatigue regime. If the calculations were made on the basis of ϵ_f' , the improvement in wear resistance of 1 Cr over Std rail would be projected to be about 100%. What is observed actually is an improvement of about 50%. Thus it appears that the available cyclic fatigue data are not sufficiently appropriate (as-rolled vs. cold worked) to provide a more precise prediction.

As EHD lubrication deteriorates, a transition to mild abrasive wear and then possibly to severe abrasive wear would be expected. Bolton, et al.,¹⁸ have observed in laboratory tests that in the mild wear regime, the logarithm of wear rate is a linear function of contact stress. From the BCL studies¹⁴ of Hertzian contact, the surface octahedral shear stresses on new rail can be shown to follow approximately the relationship

$$\log \tau_{\text{Oct}} = \log [10.55 (WL)^{0.301}] + 0.9976\mu$$

where,

WL = the wheel load in kips,

μ = the friction coefficient, and

τ_{Oct} is in ksi.

If the presumption is made that the FAST lubricated and dry regimes are characterized by friction coefficients near 0.1 and 0.5, respectively, the 19 kip wheel load contact stresses may be used to illustrate how the wear rate of different rail metallurgies will vary in two different lubrication regimes. However, the fact that the wear rates of different metallurgies are not the same at a given level of lubrication requires that a material sensitive parameter be included in the analysis. A unified relationship for all materials can be developed by incorporating Brinell hardness so that,

$$\log W = -3.4437 + 27.41 \left(\tau_{\text{oct}} / H^{2.5} \right)$$

where,

W = the gage face wear rate in inches/MGT,

τ_{oct} = the surface octahedral shear stress in ksi, and

H = the gage face Brinell hardness.

Figure 11 illustrates the agreement between observed and predicted gage face wear rates of different metallurgies tested in the current experiment in both the lubricated and unlubricated regimes. With the exception of FHT and CrMo A (unlubricated), the agreement with prediction is within 0.0010"/MGT in the unlubricated regime and 0.0002"/MGT in the lubricated regime.

The poorer-than-predicted performance of CrMo A rail may be related to its metallurgical structure; it is believed to be at least partially bainitic. Bainitic rail steels have been shown to exhibit much poorer wear resistance than do pearlitic rail steels.¹⁹ The behavior of the FHT rail is more difficult to understand. The rail has consistently exhibited poorer gage face wear resistance than its hardness would suggest that it should--even though higher carbon FHT rails were selected intentionally in the current experiment. The fact that it is processed in the mill by oil quenching followed by tempering admits to the possibility, at least, that it also may be partially bainitic.

The transition in modes is shown conceptually in Figure 12 as the friction coefficient changes. A variant on the model is a transition to severe wear for Std rail above a critical wear rate.

Wear debris collected at FAST in a previous experiment during a brief period of unlubricated running was observed²⁰ to be primarily flakes about 80 μm and 140 μm long for Std and HH rail, respectively. Bolton, et al.,¹⁸ have observed in laboratory tests that flakes of this size are found in a mild wear regime, suggesting that a wear model based on a mild wear mode may be appropriate to the unlubricated regime of FAST operations.

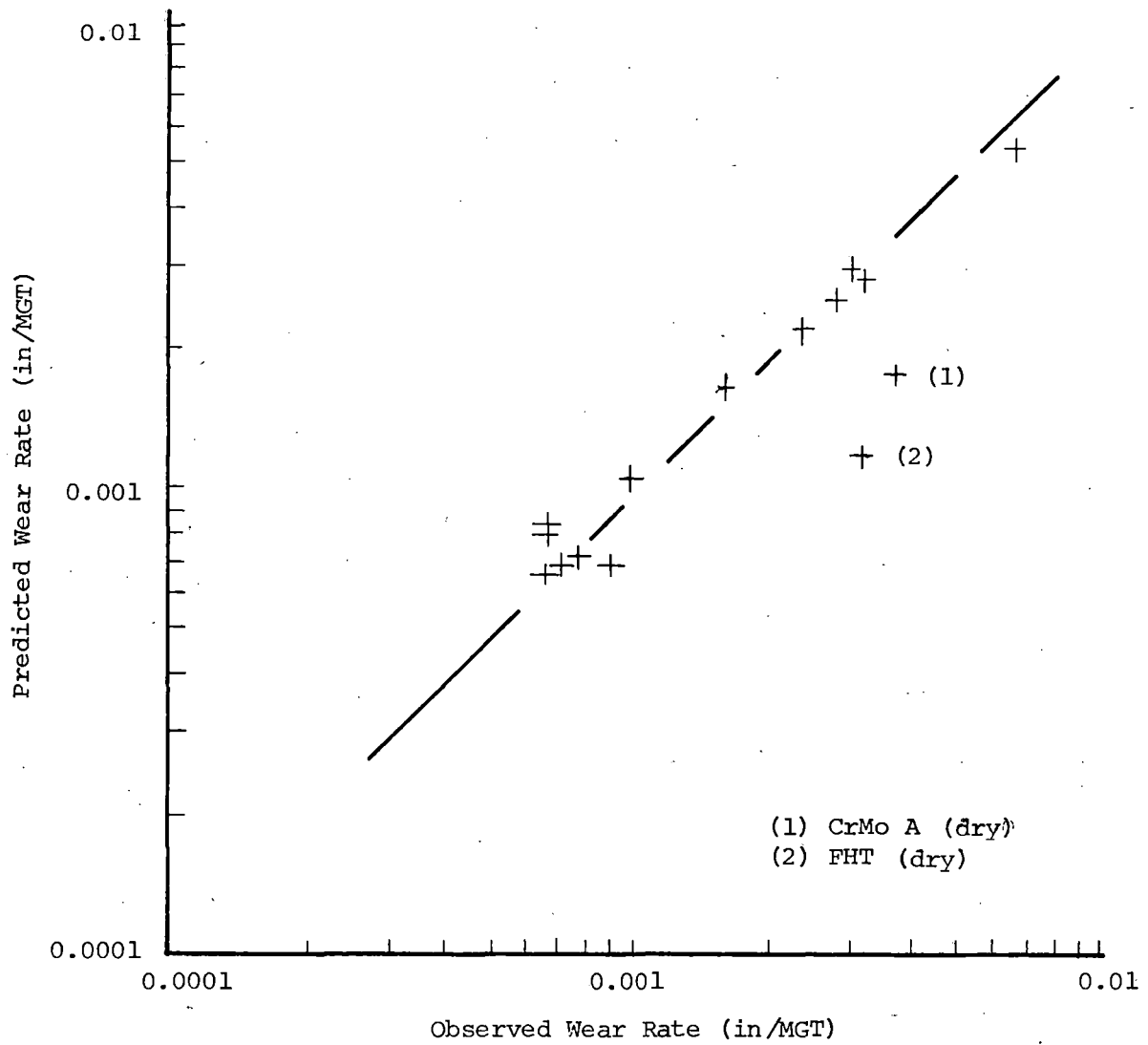


FIGURE 11. AGREEMENT BETWEEN OBSERVED AND PREDICTED WEAR RATES.

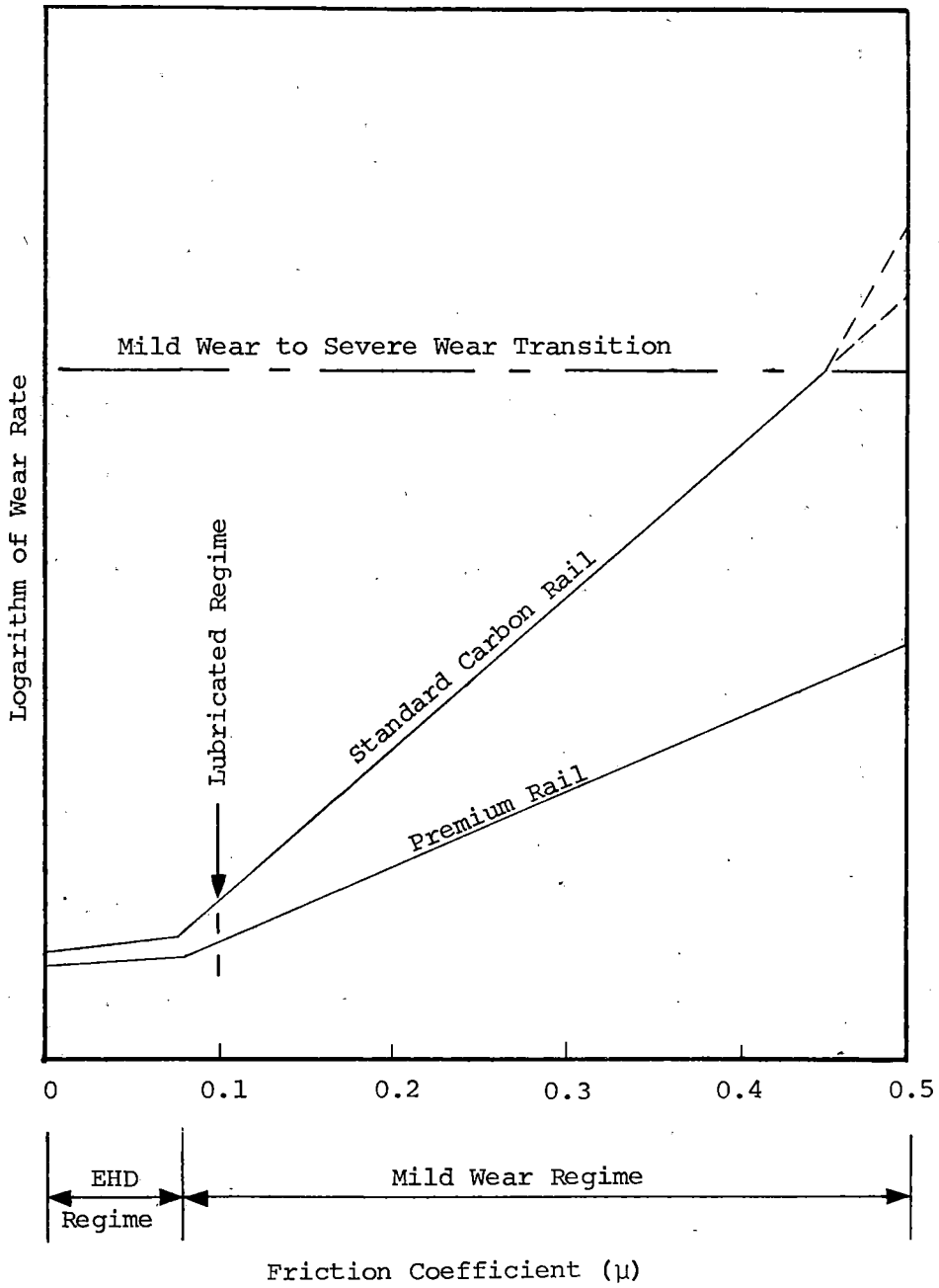


FIGURE 12. CONCEPTUAL VIEW OF CHANGE IN WEAR MECHANISM AS FRICTION COEFFICIENT CHANGES.

5.0 CONCLUSIONS

The rather strong dependence of rail and wheel wear rates upon rail to wheel hardness ratio suggests that wear mechanisms other than purely adhesive wear are active under the FAST service conditions in the unlubricated regime. Utilizing the FAST wear data in an analysis based upon observations of Rabinowicz, one would project that both improvement or deterioration of wear performance of one component might be possible by increasing the hardness of the mating component. The mechanism of wear, the relative wear rates (FM) of the component changed, and the hardness ratio of rail and wheel would determine which alternative occurs.

The strong metallurgy:lubrication interaction that has been observed to occur in rails can be understood in terms of transition from full or partial EHD lubrication to mild wear, with the possibility of severe wear occurring above a limiting value, at least for standard rail.

REFERENCES

1. Jamison, W.E., Wear of Steel in Combined Rolling and Sliding, Preprint 80-LC-5B-1, American Society for Lubrication Engineers, Park Ridge, IL.
2. Kumar, S., and Margasahayam, R., IIT Trans. 78-1, Illinois Institute of Technology, Chicago, IL, 1978.
3. Babb, A.S., Testing Techniques for Railway Materials, Research Report Prod/Eng/7063/73A, British Steel Corporation, London, England.
4. Marich, S., and Curcio, P., "Development of High Strength Alloyed Rail Steels Suitable for Heavy Duty Applications," STP 644, American Society for Testing and Materials, Philadelphia, PA, p. 188.
5. Steele, R.K., A Perspectival Review of Rail Behavior at the Facility for Accelerated Service Testing, FRA/TTC-81/07, Transportation Test Center, Pueblo, CO.
6. Allen, R.A., Radial Truck Experiment - Restart at FAST, FAST/TTC/TN-81-02, Transportation Test Center, Pueblo, CO.
7. Leary, J., Wear Characteristics of Four Wheel Types Run on Unlubricated Track, FAST/TTC/TN-DT-152, Transportation Test Center, Pueblo, CO.
8. Punwani, S.K., Cruse, W.J., et al., Facility for Accelerated Service Testing, Progress Report #2, R-288, Association of American Railroads, Chicago, IL, 1977.
9. Marich, S., and Stone, D.H., "Metallographic Examination of Cracked Wheel Flanges from FAST," Paper 5-2, Proc., Sixth International Wheelset Congress, Colorado Springs, CO. 1978.
10. Rabinowicz, E., "Wear Coefficients - Metals," Wear Control Handbook, American Society of Mechanical Engineers, New York, 1980, pp. 501-502.
11. Clayton, P., "Lateral Wear of Rails on Curves," Tribology, Inst. Mech. Eng., London, 1978, pp. 83-90.
12. Rabinowicz, E., op. cit., p. 476.
13. Steele, R.K., discussion of reference 1, to be published by American Society for Lubrication Engineers.
14. John, T.C., Davies, K.B., et al., Engineering Analysis of Stresses in Railroad Rail: Phase I, Report G6266-0101, Battelle-Columbus Laboratories, Columbus, OH, 1977.
15. Stone, D.H., and Steele, R.K., "The Effect of Mechanical Properties Upon the Performance of Railroad Rails," STP 644, American Society for Testing and Materials, Philadelphia, PA, 1976, pp. 21-48.

16. Morrow, J., "Internal Friction, Damping, and Plasticity," STP 378, American Society for Testing and Materials, Philadelphia, PA, 1965, p.45.
17. Dabell, B.J., Hill, S., and Watson, P., "An Evaluation of the Fatigue Performance of Conventional British Rail Steels," STP 644, American Society for Testing and Materials, Philadelphia, PA, 1976, pp. 430-448.
18. Bolton, P.J., Clayton, P., and McEwen, I.J., Wear of Rail and Tire Steels Under Rolling/Sliding Condition, Preprint 80-LC-5B-3, American Society for Lubrication Engineers, Park Ridge, IL.
19. Marich, S., "Research on Rail Metallurgy," Bulletin, 663, Vol. 78, American Railway Engineering Association, Chicago, IL, p. 597.
20. Rail Lubrication Studies at the Facility for Accelerated Service Testing, FAST/TTC/TN-80/08, Transportation Test Center, Pueblo, CO.

**Observations of In-Service Wear of Railroad
Wheels and Rails Under Conditions of Widely
Varying Lubrication, 1982**
US DOT, FRA, Roger K Steele (FRA/TTC-82/05)

**PROPERTY OF FRA
RESEARCH & DEVELOPMENT
LIBRARY**